Published in final edited form as:
J Immunol. 2006 October 1; 177(7): 4402–4413.

A Large T Cell Invagination with CD2 Enrichment Resets Receptor Engagement in the Immunological Synapse[1]

Kentner Singleton[2,*], **Nadia Parvaze**[2,*], **Kavyya R. Dama**[*], **Kenneth S. Chen**[*], **Paula Jennings**[*], **Bozidar Purtic**[*], **Michael D. Sjaastad**[‡], **Christopher Gilpin**[†], **Mark M. Davis**[§], and **Christoph Wülfing**[3,*,†]

[*]Center for Immunology, University of Texas Southwestern Medical Center, Dallas, TX 75390

[†]Department of Cell Biology, University of Texas Southwestern Medical Center, Dallas, TX 75390

[‡]Bio-X Program, Stanford University, and Howard Hughes Medical Institute, Stanford, CA 94305

[§]Department of Microbiology and Immunology, Stanford University, and Howard Hughes Medical Institute, Stanford, CA 94305

Abstract

T cell activation is driven by the TCR and complemented by costimulation. We have studied the dynamics of ligand-engagement of the costimulatory receptor CD2 in T cell/APC couples. Thousands of ligand-engaged CD2 molecules were included in a large T cell invagination at the center of the cellular interface within 1 min of cell couple formation. The structure and regulation of this invagination shared numerous features with phagocytosis and macropinocytosis. Three observations further characterize the invagination and the inclusion of CD2: 1) numerous ligand-engaged receptors were enriched in and internalized through the T cell invagination, none as prominently as CD2; 2) dissolution of the T cell invagination and CD2 engagement were required for effective proximal T cell signaling; and 3) the T cell invagination was uniquely sensitive to the affinity of the TCR for peptide-MHC. Based on this characterization, we speculate that the T cell invagination, aided by CD2 enrichment, internalizes parts of the TCR signaling machinery to reset T cell signaling upon agonist-mediated, stable APC contact.

T cells are activated in a cellular interaction with APCs. The central activating receptor is the TCR (1). It recognizes antigenic peptides presented by MHC on the surface of the APC. It is remarkably sensitive to small changes in the affinity of the TCR for peptide-MHC (1). Costimulatory receptor engagement complements and amplifies the TCR peptide-MHC interaction. Two of the most prominent interactions are those of CD28 with B7 and LFA-1 with ICAM-1 (2,3). Another costimulatory interaction with a hitherto unresolved function is that of CD2 (4) with its mouse ligand CD48 (2). Engagement of CD2 with pairs of stimulatory Abs can activate T cells as effectively as Ab engagement of the TCR, establishing substantial potency (5). This finding is consistent with a direct linkage of CD2 to components of the TCR signaling machinery (6–8). Proline-rich regions in the CD2 cytoplasmic domain mediate cross-

[1]This work was supported by grants from the National Institutes of Health (to C.W.) and the Howard Hughes Medical Institute (to M.M.D.).

[3]Address correspondence and reprint requests to Dr. Christoph Wülfing, Center for Immunology, University of Texas Southwestern Medical Center, 5323 Harry Hines Boulevard, Dallas, TX 75390-9093. christoph.wuelfing@UTSouthwestern.edu.
[2]K.S. and N.P. contributed equally to this work.

Disclosures
The authors have no financial conflict of interest.

talk with β_1 integrins (9) and bind to two adaptor proteins, CD2 binding protein 2 (10) and CD2 adaptor protein (11). However, CD2 deficiency has generally only modest effects on T cell activation, suggesting a limited requirement for CD2 (12). In this study we describe enrichment of CD2 in a large T cell invagination. The characterization of the T cell invaginations suggests that they, as aided by enrichment of CD2, serve to reset the proximal T cell signaling machinery upon formation of a tight T cell/APC couple.

Materials and Methods

Cells and reagents

In vitro-primed primary T cells from 5C.C7 and DO11.10 TCR transgenic mice were generated as described (13,14). The use of these mice has been reviewed and approved by the University of Texas Southwestern Medical Center Institutional Animal Care and Use Committee. As APCs, I-E^k-GFP-transfected A20 B lymphoma cells (14), A20 and CH27 B lymphoma cells, CH27 cells transfected with CD48iGFP or ICAM-1-GFP (15), or CHO cells transfected with I-E^k and CD48iGFP were used. CD48iGFP was generated by replacing the amino acids coding for the GPI membrane anchor with the transmembrane and cytoplasmic domains of ICAM-1 followed by GFP. Mature primary dendritic cells (DCs)[4] were prepared by culture of 5C.C7 bone marrow suspensions in 20 ng/ml GM-CSF and 1 ng/ml IL-4 for 6 days, followed by overnight activation with 100 ng/ml LPS (16). Retroviral transduction was as described (17). Agonist peptide concentrations were adjusted by dilution into null peptide (14). Costimulation blockade with Abs against CD48, ICAM-1, or B7-1/B7-2 was as described (14). The following Abs were used: anti-phospho LAT(Y191) (Cell Signaling Technology), anti-phosphotyrosine (4G10; Upstate Serologicals), anti-CD2 (RM2–5; BD Pharmingen), and anti-CD48 (HM48-1; BD Pharmingen).

Imaging and image analysis

The microscopy system and image acquisition have been described in detail (17). Briefly, primary T cells and peptide incubated APCs were allowed to interact at 37°C on the microscope stage. To ensure comparability with B cell lymphoma APCs, CHO cells were detached with 1 mM EDTA/PBS before imaging. Every 20 s a differential interference contrast brightfield image and 26 GFP images spaced 1 μm in the *z* plane covering the entire cell were acquired. For analysis, three-dimensional reconstructions were made. An APC extension was defined as a mostly spherical area of increased ligand (i.e., CD48iGFP, B72iGFP, I-E^k-GFP, ICAM-1-GFP) fluorescence at the center of the T cell-APC interface (>20% of the interface diameter away from the edge of the interface), where >50% of the area of accumulation was extending beyond the plane of the APC interface. All such events that occurred within the first minute of cell couple formation were scored. Later such events were not observed. The percentage of total fluorescence contained in the APC extensions was calculated from three-dimensional reconstructions by measuring the total fluorescence intensity in background-corrected top-down cylindrical volumes containing the extension or the rest of the cell. No significant differences were seen for the analysis of deconvolved vs non-deconvolved fluorescence data. CD48iGFP accumulation patterns were defined identical with MHC accumulation (14). Internal ζ-chain accumulation was defined as a spherical area of increased fluorescence (≥40% above cellular background) at the center of the interface that was removed at least 1 area diameter from the T cell-APC interface, which did not have any overlap with the APC and did not last longer than two frames (i.e., 40 s). Both tat SEC7 and tat SEC7mt were constructed, expressed in *Escherichia coli*, and purified in analogy to the previously described tat WASP VCA domain (17) using the published SEC7 inactivating mutation and domain boundaries

[4]Abbreviations used in this paper: DC, dendritic cell; DLC1, dynein L chain 1; EM, electron microscopy; LAT, linker of activated T cells; MCC, moth cytochrome *c*; Pak, p21-activated kinase.

(18). The tat dynein L chain 1 (DLC1) peptide was the same as published (19) with the exception of a disulfide bond linking the tat and the DLC1 moieties instead of a peptide bond. The tat SEC7mt and tat DLC1 were used at the indicated concentrations as previously described (17). Briefly, the T cells were preincubated for 30 min at 37°C with the tat fusion reagent, and the reagent was present during the T cell to APC interactions at the same concentration. Images to be deconvolved were acquired similar to standard fluorescence microscopy on a Deltavision Deconvolution microscope with a ×60 oil immersion objective (Applied Precision Instruments). The 90 z planes spaced 0.25 μm and a brightfield image were acquired every minute. For spinning disk confocal microscopy, 41 z planes spaced 0.4 μm were acquired every 30 s on a PerkinElmer Ultraview ERS microscope, using a ×63 oil immersion objective. Red and green fluorescence images were acquired immediately one after the other at each z plane. For homogeneous cell labeling, DCs or T cells were incubated with 2 μM SNARF AM ester or 2 nM CFSE (both Molecular Probes) for 10 min at room temperature. For anti-CD2 staining, T cells and APC interacted at 37°C for 5 min before either direct staining with 2 μg/ml PE-conjugated anti-CD2 on ice in the presence of 10 μg/ml Fc block or the cell couples were fixed with formaldehyde according to standard protocols (20) first.

For two-color three-dimensional imaging, an actin-mCherry (21) fusion protein was generated and retrovirally expressed as actin-GFP (17). During image acquisition, both red and green images were acquired at each z plane before moving to the next plane. Excitation filters were rapidly changed with the DJ5 filter changer (Sutter Instruments), z planes with a piezoelectric element (Physik Instrumente). The same dichroic mirror and emission filter were used for both colors. There was no significant bleed-through between the colors using this setup. Use of the dual-color dichroic reduced fluorescence intensity. Therefore, only 11 z planes spaced 2 μm were acquired with an acquisition time of 1 s per color and z plane (vs 200 ms in the single-color experiments). Thirty-one time points 30 s apart were acquired. Simultaneous two-color imaging thus resulted in moderate loss of temporal and spatial information. Analysis was as in the single-color experiments.

For electron microscopy (EM), 10×10^6 T cells and 5×10^6 APCs were washed free of serum, gently spun together, and incubated as a cell pellet for 2 min at 37°C before processing according to standard procedures. Briefly, cells were fixed with ice-cold 2% glutaraldehyde in 0.1 M caco-dylate buffer, postfixed in 1% osmium tetroxide in 0.1 M cacodylate buffer, stained with 1% aqueous uranyl acetate, dehydrated, and embedded in EMBED 812. Grids were analyzed blind. Images were acquired at a magnification of ×20,000. A T cell invagination was defined as T cell membrane pointing into the T cell so that either the depth of the invagination was larger than its maximal width or so that the width inside the T cell was larger than the width at the T cell surface. No T cell invaginations were observed in the absence of agonist peptide.

The statistical significance of differences between conditions that were analyzed as a percentage of cell couples with a particular phenotype was determined using a two-sample proportion *z* test.

Effector functions and fluid phase uptake

Linker of activated T cells (LAT) and TCR-ζ phosphorylation were determined by Western blot analysis of cell extracts from T cell/APC couples that interacted for 5 min, as previously described (13). To measure T cell fluid phase uptake, T cell/APC couples interacted for 10 min in the presence of fluorescein at 37°C, were washed on ice, and fluorescein contents of T cells bound to APCs only was determined by fluorescence microscopy. T cell intracellular calcium concentrations were determined by flow cytometry. 5C.C7 T cells were loaded with 1 μM Indo-1-AM ester (Molecular Probes) and CH27 APC were incubated with 10 μM moth cytochrome *c* (MCC) peptide and loaded with 0.5 μM SNARF AM ester. T cells and APC

were prewarmed separately to 37°C, gently spun together for 30 s, and immediately analyzed by flow cytometry. T cell/APC couples were identified by larger size and increased Indo-1 and SNARF fluorescence. Tat SEC7 domain guanine nucleotide exchange factor activity for Arf6 was determined in vitro using purified tat SEC7 and recombinant myristoylated Arf6 (22) according to standard procedures (23).

Results

CD2/CD48 accumulates at the T cell-APC interface

Knowledge of the spatiotemporal patterns of receptor engagement can contribute substantially to the elucidation of receptor function. To assess the localization of CD2/CD48 during T cell activation, we constructed a CD48-GFP fusion protein. CD48 is a GPI-linked receptor and the functionality of CD2/CD48 depends critically on the combined size of their extracellular domains (24). So as to not change the CD48 extracellular domain size by fusion to GFP, we substituted the CD48 GPI membrane anchor with the transmembrane and cytoplasmic domains of ICAM-1 C terminally fused to GFP (CD48iGFP). In B cell lymphoma APCs, as used in this model, ICAM-1-GFP localization was exclusively driven by ligand binding (15), establishing that the ICAM-1 transmembrane and cytoplasmic domains do not provide a localization signal by themselves. The 5C.C7 TCR recognizes the MCC 92–103 peptide presented by I-E^k. We studied the interaction of live, in vitro primed, primary 5C.C7 TCR transgenic T cells with CH27 B cell lymphoma APCs, transfected with the CD48iGFP construct. In the presence of 10 μM MCC peptide, a “full stimulus,” CD48iGFP accumulated within seconds at the T cell-APC interface (Fig. 1*A* and shown in supplemental video 1)[5] in 78% of the T cell/APC couples (n = 158). In 82%, couples displayed accumulation at the center of the interface. Pretreatment of the APC with 2 μM cy-tochalasin D to block active CD48iGFP localization did not interfere with its interface accumulation (data not shown), confirming that CD48iGFP interface accumulation was indeed driven by binding to a ligand on the T cell. All 5C.C7 T cells expressed CD2, some also expressed an alternate CD48 ligand, 2B4 (data not shown). Staining of fixed or live chilled 5C.C7 T cell/CH27 APC couples with anti-CD2 Abs showed the same central pattern as CD48iGFP (Fig. 1*B*). Moreover, when fixed after 5 min of T cell-APC contact in the presence of a full stimulus (10 μM MCC peptide), 76% of the cell couples (n = 59) showed interface accumulation of CD2, 89% of those at the center of the interface, similar to the CD48iGFP live cell data. Staining with anti-2B4 did not show interface accumulation. CD48iGFP thus reported CD2-driven accumulation of CD2/CD48 at the T cell-APC interface. Using human T cell clone-APC combinations or murine primary T cells on supported lipid bilayers as APC substitutes, accumulation of CD2/CD48 has previously been demonstrated, whether in a central pattern or spread over the interface (11,25).

The most intriguing aspect of CD2/CD48iGFP localization, however, was its inclusion in a large T cell invagination, as described in this study. Next, we characterize the structure, composition, and regulation of this invagination (as displayed in Figs. 1–6). To assess its function, one ideally would like to block its formation without impeding other features of T cell organization and T cell signaling. Reagents to accomplish this effect are currently not available. As an alternate approach, we will therefore relate the formation of the T cell invagination to various elements of T cell activation (as displayed in Figs. 7 and 8). Such correlations will allow us to generate hypotheses about the function of the T cell invagination, a first step toward causality.

[5]The online version of this article contains supplemental material.

Characterization of the T cell invagination with fluorescence microscopy

During the activation of 5C.C7 T cells by CH27/CD48iGFP APCs in the presence of a full stimulus (10 μM MCC peptide), CD48iGFP fluorescence could be seen extending from the APC surface into the T cell selectively at the center of the interface within the first minute of T cell-APC contact (Fig. 1*A*, supplemental data). This result was seen in 69% of the cell couples ($n = 166$). We call this phenomenon an APC extension. Deconvolution microscopy confirmed that CD48iGFP could reach deep into the T cell (Fig. 1*C*). To assess whether APC extensions were matched by T cell invaginations, we labeled T cells homogenously with the red dye SNARF and performed spinning disk confocal microscopy of CH27/CD48iGFP SNARF-labeled 5C.C7 T cell couples. In the presence of a full stimulus (10 μM MCC peptide), APC extensions were found in 68% ($n = 28$) of the cell couples, all of which showed matching T cell invaginations (Fig. 2). To assess whether T cell invaginations also occurred when T cells were activated with other APCs, we generated bone marrow-derived mature DCs from 5C.C7 mice. We labeled the DCs homogeneously with CFSE and used them to activate SNARF-loaded 5C.C7 T cells. In the presence of a full stimulus (10 μM MCC peptide), DC extensions with matching T cell invaginations were observed in 62.5% ($n = 16$) of the cell couples (Fig. 3). To investigate whether T cell invaginations could also be observed using receptors on the T cell surface, we used a TCR ζ-GFP fusion protein. The TCR ζ-chain is of interest, as it can be immunoprecipitated and cocapped with CD2 (7). We used primary, in vitro primed DO11.10 T cells retrovirally transduced with ζ-chain-GFP (26). The DO11.10 TCR recognizes the OVA peptide 324–340 presented by I-A^d. In 28% of cell couples ($n = 47$) between DO11.10 T cells and A20 B cell lymphoma APCs incubated with 10 μM OVA peptide, a full stimulus, transient ζ-chain-GFP accumulation below the center of the T cell-APC interface was apparent within 1 min of cell couple formation (Fig. 1*D* and supplemental video 2). The percentage of occurrence matched that of MHC class II APC extensions, as determined using 5C.C7 T cells and I-E^k-GFP-transfected A20 APCs (20.5%; $n = 39$). Higher magnification, spinning disk confocal microscopy demonstrated that TCR ζ-chain-GFP lined the sides of the T cell invagination and was enriched at its bottom (Fig. 1*E*). In summary, T cell invaginations with matching APC extensions could be visualized by labeling ligands on the APC, entire APCs, entire T cells, and receptors on the T cell.

Characterization of the T cell invagination via EM

For a higher resolution of APC extension-T cell invaginations, we fixed primary T cell-B cell lymphoma APC couples after 2 min of interaction and processed them for EM. Establishing generality, various combinations of TCR transgenic primary T cells, 5C.C7 or DO11.10, with CH27 and A20 APCs, untransfected or transfected with I-E^k-GFP or CD48iGFP, were used with only small differences. Between 10 and 22% of cell couples (average of 16%; $n = 360$), showed a membrane invagination of the T cell at the center of the interface with tight T cell-APC membrane contact (Fig. 4*A*). The smaller A20 APC allowed fewer T cell invaginations, possibly because they had less membrane mass to provide. The lower percentage of T cell invaginations detected by EM in comparison to the CD48iGFP fluorescence extensions observed by live cell microscopy is consistent with the lack of temporal resolution and the restriction to one 80-nm thin slice in the EM samples.

We quantified the size of T cell invaginations from the electron micrographs. Although their size varied substantially, they were at least 1-μm deep or wide, suggesting a structure with an area of 1 μm^2 or wider. This finding is consistent with their visibility and shape observed in the fluorescence images. For a semiquantitative estimate of the number of receptor/ligand couples in the T cell invaginations, we determined ligand fluorescence enrichment. Although the total number of CD48iGFP molecules on the APC surface was not quantified, comparison of fluorescence intensities with I-E^k-GFP-transfected cells where such an analysis has been performed (14) suggests a total number of CD48iGFP molecules between 50,000 and 100,000

per CH27 APC. A 3.7 ± 2.5% of total CD48iGFP fluorescence was contained in the extensions. This corresponds to ~3000 molecules of CD48iGFP and, by implication, CD2 itself. In summary, fluorescence and EM data establish a deep invagination into the T cell, with bound APC membrane, at the center of the T cell-APC interface, immediately following cell couple formation that contains hundreds to thousands ligand-engaged receptor molecules.

Characterization of T cell invaginations via CD2/CD48 enrichment

To assess the composition of T cell invaginations, we determined the occurrence of APC extensions using CH27 cells transfected with B72iGFP (13), ICAM-1-GFP (15), or A20 cells transfected with I-E^k-GFP (14). All APCs triggered APC extensions in 20–40% of the T cell/APC couples, suggesting that in addition to CD2/CD48, TCR/MHC, LFA-1/ICAM-1, and CD28/CTLA-4/B7 were present in T cell invaginations. However, in comparison to CD48iGFP (69% of cell couples with APC extensions), the occurrence of APC extension was significantly ($p < 0.001$) lower for all other GFP-tagged APC surface proteins.

To assess whether CD2 can regulate the formation of T cell invaginations, we manipulated CD48 expression on the APCs. Using CH27 APCs, CH27 cells transfected with CD48iGFP, or CH27 APCs in the presence of 10 μg/ml blocking anti-CD48 Abs, the frequency of T cell/APC couples with T cell invaginations as observed by EM varied insignificantly from 19 to 22% (Fig. 4*B*). CD2/CD48 engagement thus did not regulate the formation of T cell invaginations. Furthermore, we transfected CHO cells with I-E^k and CD48iGFP. CD48iGFP levels were comparable to trans-fected CH27 cells. CD48iGFP-labeled APC extensions were only observed in 9% of the cell couples as opposed to 69% with trans-fected CH27 cells. CD2/CD48 engagement thus was not sufficient to promote T cell invaginations, further arguing against a regulatory role. As CD2/CD48 did not regulate the formation of T cell invaginations, the increased frequency of CD48iGFP-labeled APC extensions as compared with those with other receptor/ligand pairs argues for CD2/CD48 enrichment in T cell invaginations.

Characterization of the T cell invagination as regulated similar to macropinocytosis and phagocytosis

As an additional means of characterization and to generate reagents to interfere with T cell invaginations, we studied the regulation of their formation and dissolution. The formation of the T cell invagination was driven by the T cell. Blocking APC cytoskeletal dynamics, as would be required for active protrusion of APC extensions, with cytochalasin D did not interfere with T cell invaginations (C. Wülfing, unpublished data). However, interference with a key element of T cell signaling, the elevation of the intracellular calcium concentration, did interfere with T cell invaginations. Treatment of 5C.C7 T cells with 20 μM BAPTA and 5 mM Ni^{2+} in the presence of a full T cell stimulus (10 μM MCC peptide) resulted in no 5C.C7/CH27-CD48iGFP cell couples ($n = 24$), displaying an CD48iGFP APC extension ($p < 0.001$ vs buffer only). Cell couple formation itself was undisturbed.

The morphology of T cell invaginations resembles intermediate stages of two endocytic events that can enclose large volumes of extracellular space, macropinocytosis (27,28) and phagocytosis (29). To assess a potential endocytic nature of T cell invaginations, we interfered with Arf6, a critical regulator of endosome trafficking (30). Interference with Arf6 activity blocks recycling of endosomes to the plasma membrane leading to their enlargement. Consequently, uptake of new endosomes is slowed. Arf6 activity is required for phagocytosis (31) and likely macropinocytosis (32). In the rest of this paragraph, we characterize a reagent to interfere with Arf6 activity in primary T cells. In the next paragraph, we describe its application. T cells use cytohesin-1 as a guanosine exchange factor to activate Arf6 (33). To interfere with Arf6 activation, we used a dominant-negative mutant of the SEC7 guanosine exchange factor domain of cytohesin-1 (18), made membrane-permeable using protein

transduction (34), which is called tat SEC7mt. In protein transduction, the addition of a 10 amino acids peptide derived from the HIV tat protein confers membrane permeability on a protein, allowing short-term and quantitative uptake into cells. The isolated wild-type cytohesin-1 SEC7 domain enhances Arf6 GTP-loading (35). To assess the functionality of the tat-linked version of this domain (tat SEC7), we assessed in vitro Arf6 GTP-loading with purified proteins (Fig. 5*A*). The 1 μM tat SEC7 increased Arf6 GTP-loading by 280% over buffer only, and tat SEC7mt by 20%. The enhancement was specific for Arf6, as 1 μM tat SEC7 did not enhance RhoA GTP-loading. These data thus establish functionality of the tat-linked SEC7 domain. Tat SEC7mt-mediated interference with in vivo Arf6 GTP-loading should lead to endosome enlargement in 5C.C7 T cells. To test this hypothesis, we assayed fluorescein uptake into APC-bound T cells. The 3 μM tat SEC7mt significantly ($p < 0.05$) enhanced fluid phase fluorescein uptake by 55%, consistent with endosome enlargement (Fig. 5*B*). None of five other tat fusion proteins tested (tat WASP VCA (17), N17 dominant-negative Rac1 (36), N17 dominant-negative Cdc42 (36), the WASP GTPase-binding domain (37), or V12 constitutively active Cdc42 (36)) showed a significant enhancement, establishing specificity. Cytohesin-1 has been linked to the regulation of LFA-1 avidity (18). To test whether tat SEC7 or tat SEC7mt regulate LFA-1 avidity, we studied the interaction between 5C.C7 T cells and CHO cells that had been transfected with I-E^k and ICAM-1-GFP (CHO/I-E^k/ICAM-GFP). In this interaction, ICAM-1 clustering is only seen when LFA-1 is activated pharmacologically by treating T cells with PMA. ICAM-1 clustering thus serves in this model as a direct indication of the up-regulation of the LFA-1 avidity (Fig. 5*C*). In the presence of CHO/I-E^k/ICAM-GFP APCs, 10 μM MCC peptide (a full stimulus), and 150 nM PMA, 61% of cell couples showed ICAM-1 accumulation at all time points analyzed (1, 3, 5, and 7 min after cell couple formation); 10% of cell couples were without accumulation. In contrast, in the absence of additional PMA, no cell couples showed ICAM-1 accumulation at all time points ($p < 0.001$ vs PMA addition), and 91% did not show any accumulation ($p < 0.001$). Tat SEC7mt did not interfere with the PMA-dependent LFA-1 avidity up-regulation (Fig. 5*C*). In the presence of CHO/I-E^k/ICAM-GFP APCs, 10 μM MCC peptide, 150 nM PMA, and 3 μM tat SEC7mt, 57% of the cell couples showed ICAM-1 accumulation at all time points, 11% were without accumulation (Fig. 5*C*). Furthermore, wild-type tat SEC7 could not trigger LFA-1 avidity up-regulation. After 15 min of 5C.C7 T cell interaction with CHO/I-E^k/ICAM-GFP cells in the presence of a full stimulus (10 μM MCC peptide), 62% of the cell couples showed ICAM-GFP clustering in the presence of 150 nM PMA, 11% upon addition of buffer only ($p < 0.001$), and 6% in the presence of 2 μM tat SEC7 ($p < 0.005$) ($16 \leq n \leq 28$ cell couples). In addition, we have corroborated a lack of an effect of 3 μM tat SEC7mt on LFA-1/ICAM-1 clustering using CH27 APCs that had been transfected with ICAM-1-GFP. In the presence of a full stimulus (10 μM MCC peptide) and 3 μM tat SEC7mt, 94% of T cell/APC couples showed ICAM-1 clustering at the T cell-APC interface. The remainder showed changed ICAM-1 patterns at the interface without an increase in ICAM-1 density. Similar LFA-1/ICAM-1 clustering was seen in the absence of 3 μM tat SEC7mt and has been described previously (15). In summary, we have demonstrated enhancement of in vitro Arf6 GTP-loading by tat SEC7, increased fluorescein retention in APC-bound 5C.C7 T cells in the presence of tat SEC7mt, indicative of endosome enlargement, and lack of an effect of tat SEC7/tat SEC7mt on the avidity regulation of LFA-1. Tat SEC7mt thus exerts its effects most likely through regulation of the Arf6-dependent endosome recycling.

Addition of 3 μM tat SEC7mt to 5C.C7 T cell to CH27-CD48iGFP interactions in the presence of a full stimulus (10 μM MCC peptide) reduced the occurrence of CD48iGFP extensions significantly ($p < 0.005$) to 36% of the cell couples (vs 69% with buffer only), suggesting an involvement of the T cell endocytic machinery in the formation of T cell invaginations. Irrespective of the exact cellular mechanism of action of tat SEC7mt, this reagent can serve to interfere with the formation of T cell invaginations.

To further investigate the regulation of T cell invaginations and assess similarities with macropinocytosis and phagocytosis, we blocked PI3K activity that is required for both phagocytosis (38,39) and macropinocytosis (40). Using 100 nM wortmannin in the presence of a full stimulus (10 μM MCC peptide) significantly blocked ($p < 0.001$) APC extensions in 5C.C7 T cell to CH27-CD48iGFP interactions (26% of T cell/APC couples with CD48iGFP APC extensions vs 69% with buffer only). In addition, we blocked the p21-activated kinase (Pak) to DLC1 interaction with a DLC1-derived dominant-negative peptide as a protein transduction reagent at 1 μM (tat DLC1). The 1 μM tat DLC1 blocked the uptake of high m.w. dextran by macropinocytosis in fibroblasts and breast cancer cells (19). A 1 μM tat DLC1 in the presence of a full stimulus (10 μM MCC peptide) did not interfere with effective formation of T cell invaginations, as 77% of the cell couples displayed them. On the contrary, it stabilized the formations. The average duration of CD48iGFP extensions in 5C.C7/CH27-CD48iGFP cell couples increased significantly ($p < 0.005$) from 0.65 ± 0.35 min to 1.65 ± 1.1 min. The amount of CD48iGFP fluorescence contained in the APC extensions in these cell couples increased significantly ($p = 0.01$) from 3.7 ± 2.5 to 8.9 ± 6.3% of total CD48iGFP fluorescence. None of these effects were seen with the tat peptide in isolation (C. Wülfing, unpublished data). Stabilization of the invaginations was also evident in their significantly ($p < 0.05$) increased frequency in EM (Fig. 4*B*). These data suggest that the Pak to DLC1 interaction was required to resolve T cell invaginations, similar to its role in macropinocytosis. However, the C terminus of DLC1 that is included in tat DLC1 can also interact with other proteins (41), thus making other mechanisms of tat DLC1 action conceivable. Intriguing among the other interacting proteins is dynamin 2 (42), as it regulates actin accumulation at the T cell-APC interface (43). Changed actin dynamics are thus a prominent potential alternative for the mechanism of tat DLC1 function in the suppression of the dissolution of the T cell invaginations. To address this potential alternate mechanism, we tested whether early actin dynamics, the spreading of actin to the edges of the T cell-APC interface upon its formation (lamellipodial actin spreading, (17) as further investigated below), was sensitive to tat DLC1. In the presence of a full stimulus (10 μM MCC agonist peptide) and 1 μM tat DLC1, 86% of cell couples ($n = 28$) showed lamellipodial actin spreading, similar to a full stimulus only (82%, similar to previous data (17)). Sustained actin accumulation was equally unaffected (data not shown). An effect of 1 μM tat DLC1 on T cell invaginations through interference with dynamin function in T cell actin regulation was thus unlikely. Irrespective of the exact cellular mechanism of action of tat DLC1, this reagent can serve to stabilize T cell invaginations.

Characterization of the T cell invagination as lamellipodial actin spreading needs to precede T cell invaginations

Actin polymerization is required for the formation of phagosomes and macropinosomes. In T cell activation, actin spreads to the edges of the T cell-APC interface upon its formation (lamellipodial actin spreading) (17), suggesting that actin may have to clear at the center to allow the formation of the T cell invagination. We therefore analyzed actin dynamics and CD48/CD2 localization simultaneously. We used an actin-mCherry fusion protein introduced into 5C.C7 T cells by retroviral transduction and CH27 APCs transfected with CD48iGFP. In the presence of a full stimulus (10 μM MCC peptide), 75% of the cell couples ($n = 44$) displayed lamellipodial actin spreading, as similarly seen using an actin-GFP fusion protein (76% of cell couples) (17). Seventy-three percent of the cell couples showed early transient CD48iGFP accumulation in a central pattern, 55% a detectable APC extension. We suggest that the moderately reduced incidence of observable APC extensions was the consequence of changed imaging modalities to accommodate two colors simultaneously (see *Materials and Methods*). Lamellipodial actin spreading preceded central CD48iGFP accumulation and APC extensions (Fig. 6). In cell couples that showed lamellipodial actin spreading, 85% also showed early central CD48iGFP accumulation, and 64% a CD48iGFP APC extension. In cell couples without lamellipodial actin spreading, only 35% of the cell couples showed early central

CD48iGFP accumulation ($p < 0.01$ vs cell couples with lamellipodial actin spreading), only 27% a CD48iGFP APC extension ($p = 0.08$). These data suggest that lamellipodial actin spreading is required for the formation of CD48iGFP APC extensions. Cdc42 regulates lamellipodial actin spreading (37) as well as phagocytosis (38) and macropinocytosis (44). When we blocked lamellipodial actin spreading with 100 nM dominant-negative Cdc42 as a protein transduction reagent (Cdc42dn) (37), only 31% of the T cell/APC couples showed CD48iGFP APC extensions as opposed to 69% with buffer only ($p < 0.001$). As a control, 100 nM Rac1dn interfered neither with lamellipodial actin spreading (37) nor with CD48iGFP membrane extensions (67% of the cell couples displayed them). In summary, lamellipodial actin spreading preceded T cell invaginations, and occurrence of T cell invaginations was more frequent in cell couples with lamellipodial actin spreading, and Cdc42dn interfered with both lamellipodial actin spreading and T cell invaginations. Together, these data suggest that lamellipodial actin spreading facilitates the formation of T cell invaginations.

We thus have shown that the regulation of the formation and dissolution of T cell invaginations shares numerous features with macropinocytosis and phagocytosis, suggesting that the T cell invaginations are a related structure, as further discussed below. Interestingly, uptake of substantial amounts of fluorescence from APC extensions was not observed (Fig. 1*A*, supplemental data), suggesting that either T cell invaginations did not close but rather reverted with the APC membrane attached, or that membrane tension forced the APC cell membrane to detach from the T cell surface before closure of T cell invaginations.

Relations to T cell activation as CD2 is removed from the center of the T cell-APC interface concomitant with the dissolution of T cell invaginations

If T cell invaginations closed to form a large endocytic structure, they would be expected to remove receptors from the center of the T cell-APC interface. We, therefore, analyzed the dynamics of central receptor/ligand couple accumulation. We focused on CD2/CD48, as it was enriched in T cell invaginations, and on TCR/MHC as the central regulator of T cell activation. First, we compared central receptor/ligand couple accumulation early in the formation of T cell invaginations, as measured by the frequency of APC extensions, and following it at 1 min after cell couple formation. In the presence of a full T cell stimulus (10 μM MCC peptide), the percentage of T cell/APC couples with central CD2/CD48 accumulation dropped significantly from 69 to 47% ($p < 0.005$). These data establish a substantial loss of CD2/CD48 from the center of the T cell-APC interface over the time course of the formation and dissolution of T cell invaginations.

To assess whether T cell invaginations were causally linked to reductions in central CD2/CD48 accumulation, we interfered with their formation using 3 μM tat SEC7mt or stabilized them with 1 μM tat DLC1. Upon addition of 3 μM tat SEC7mt to a full T cell stimulus (10 μM MCC peptide), the percentage of T cell/APC couples with central CD2/CD48 accumulation was stable at 36%, the percentage with central TCR/MHC accumulation increased dramatically from 16 to 58% ($p < 0.001$) (Fig. 7). Similarly, upon addition of 1 μM tat DLC1, the percentage of T cell/APC couples with central CD2/CD48 accumulation was stable within the first minute of cell couple formation at 77 and 83% (Fig. 7). Impairing the formation of T cell invaginations or stabilizing them thus prevented the reduction of CD2/CD48 accumulation at the center of the T cell-APC interface. Impairing the formation of T cell invaginations allowed increased central TCR/MHC accumulation. This result suggests substantial internalization of CD2 and the TCR through T cell invaginations, consistent with the ~3000 molecules of CD2 likely included in an invagination and the TCR ζ-chain localization at the bottom of the invaginations (Fig. 1*E*). This reduction was specific for the center of the T cell-APC interface, as overall CD2 surface expression, as determined by FACS, was not significantly changed over the time course of T cell activation (P. Jennings and C. Wülfing, unpublished data).

Relations to T cell activation as CD2 engagement and dissolution of the T cell invaginations are required for effective proximal TCR signaling

CD2 is linked to the TCR signaling machinery (6–8). Receptor internalization in T cell invaginations including CD2 would remove parts of the TCR signaling machinery from the center of the T cell-APC interface. We hypothesize that this response might serve to reset T cell signaling upon T cell/APC couple formation to allow enhanced efficiency of subsequent signaling in persistent T cell/APC couples. If that was true, proximal T cell signaling at a time shortly after dissolution of the invaginations should be diminished if the dissolution of T cell invaginations was blocked, as resetting of T cell signaling would be impeded. A comparable effect of a blockade of the CD2 to CD48 interaction would support a role of CD2 in resetting TCR signaling through T cell invaginations. We therefore assayed phosphorylation of the adaptor protein LAT (45) and of the TCR ζ-chain 5 min after cell couple formation. Blocking the resolution of T cell invaginations with1 μM tat DLC1 in the interaction of 5C.C7 T cells with CH27 APCs in the presence of a full stimulus (10 μM MCC peptide) reduced LAT phosphorylation by 60% and that of the TCR ζ-chain by 71% (Fig. 8*A*). Blocking the CD2 to CD48 interaction with anti-CD48 Abs similarly reduced LAT phosphorylation by 37–50% using A20/I-E^k-GFP or CH27 APCs and 10 or 1 μM MCC agonist peptide (Fig. 8, *A* and *B*). The reduction was specific, as blocking LFA-1/ICAM-1 or CD28/B7 did not interfere with LAT phosphorylation (Fig. 8*B*). Similarly, blocking CD48 reduced 5C.C7 T cell ζ-chain phosphorylation by 53% using CH27 APCs and 10 μM MCC (Fig. 8*A*). These data suggest a role of T cell invaginations in the regulation of proximal T cell signaling immediately after cell couple formation. Comparable relations between efficient proximal TCR signaling on one side and CD2 engagement and dissolution of T cell invaginations on the other are consistent with the suggestion that inclusion of CD2 in the invaginations is important in this regulation of proximal T cell signaling.

To assess whether T cell invaginations affect more distal T cell signaling, we studied the elevation of the T cell intracellular calcium concentration by flow cytometry (Fig. 8*C*). In the presence of a full T cell stimulus (10 μM MCC peptide), blocking CD48 reduced the elevation of the T cell intracellular calcium concentration significantly ($p \leq 0.05$) by 18–46% at all time points within 5 min of T cell/APC couple formation (Fig. 8*D*). However, this effect was no longer specific for a CD48 blockade, as a B7 blockade showed comparable effects. Moreover, blocking the dissolution of T cell invaginations with 1 μM tat DLC1 did not have an effect (Fig. 8*D*). A role of T cell invaginations in signaling thus was limited to proximal events. Furthermore, although CD2 inclusion in the invaginations may well be significant for its function, CD2 had additional functions independent of the invaginations.

Relations to T cell activation as T cell invaginations are uniquely sensitive to the affinity of the TCR for peptide-MHC

Finally, we investigated the occurrence of T cell invaginations under various physiological T cell activation conditions, a 10-fold reduction in the concentration of agonist peptide or blockade of the costimulatory ligands ICAM-1 and B7. Although these treatments reduce IL-2 secretion by 40–60% (13), T cell invaginations were undisturbed (67, 80, and 63% of CH27/CD48iGFP-5C.C7 cell couples with APC extensions vs 69% in control). Interestingly, however, reducing the affinity of peptide-MHC for the TCR by using the MCC variant T102S (46) significantly reduced ($p < 0.001$) the formation of T cell invaginations (16% of CH27/CD48iGFP-5C.C7 cell couples with APC extensions) while only reducing IL-2 secretion to an extent that was comparable to the other treatments (C. Wülfing, unpublished data). T cell invaginations thus were uniquely sensitive to TCR affinity, suggesting that they could play a role in the differentiation between high and lower affinity TCR ligands.

Discussion

In this study we have characterized a large T cell invagination at the center of the T cell-APC interface within 1 min of its formation. It contained hundreds to thousands of various receptors with their APC membrane-embedded ligands still bound. CD2/CD48 were enriched. Membrane internalization at the T cell-APC interface in the form of transfer of APC membrane-embedded ligands for the TCR and CD28 to the T cell is well established (47,48). However, T cell invaginations are distinct. Previously described ligand transfer was not limited to the first minute after cell couple formation but occurred over hours. A large structure mediating the transfer was not found. Transfer of APC membrane to the T cell was clearly demonstrated, whereas APC membrane is likely to detach from the T cell invaginations before their closure. Rather than resembling these membrane transfer processes, T cell invaginations were similar to macropinocytosis and phagocytosis. An actin movement toward the edge of the interface with concomitant clearing of actin at the center preceded and likely facilitated T cell invaginations, similar to the actin-driven membrane extensions in macropinocytosis and phagocytosis. The formation of T cell invaginations depended on Arf6 and the rise in the T cell intracellular calcium concentration. Arf6 is required for the membrane insertion of recycling endosomes and critical in phagocytosis (31) and macropinocytosis (32). Elevations in the intracellular calcium concentration play a central role in exocytosis in nonsecretory cells (49), including the insertion of cell membrane mass by exocytosis before the formation of phagosomes (50). PI3K and Cdc42 activity were required for T cell invaginations, similar to phagocytosis (38,39) and macropinocytosis (40,44). Finally, the interaction of Pak with DLC1 was required to resolve T cell invaginations, consistent with a role of this interaction in the regulation of macropinocytosis (19). Together these data suggest a mechanism, in which motion of actin toward the edge of the forming T cell-APC interface with concomitant clearing of the center and calcium- and Arf6-dependent exocytosis precede the formation of large endocytic T cell invagination whose closing is dependent on the activation of dynein motor proteins by Pak. The invaginations were triggered by contact with the APC membrane and could pull APC membrane in, thus initially resembling phagocytosis. However subsequently, APC membrane detached before closure of the invaginations, thus leaving them to enclose only liquid, which more resembled macropinocytosis at this later stage.

To conclusively elucidate the function of T cell invaginations, specific interference with their formation without affecting other elements of cellular organization and signaling would be required. Reagents to accomplish this effect are currently unavailable. We therefore can only speculate on the function of T cell invaginations based on their characteristics. We describe three such characteristics in this study: CD2/CD48 and TCR/MHC were removed from the center for the T cell-APC interface on the time scale of the formation and dissolution of the invaginations; proximal T cell signaling was similarly reduced upon interference with the dissolution of the invaginations and reduced CD2 engagement; and the formation of T cell invaginations was particularly sensitive to the affinity of the TCR for peptide-MHC. Based on these characteristics, we speculate that T cell invaginations mediate resetting of the proximal T cell signaling machinery through receptor internalization upon cell couple formation. Such resetting might allow subsequent signaling to occur more efficiently. As CD2 is linked to the TCR signaling machinery, the reductions in CD2 levels concomitant with the dissolution of T cell invaginations potentially removes parts of the TCR signaling machinery from the center of the T cell-APC interface immediately after its formation. Supporting an association of CD2 with the TCR signaling machinery throughout endocytic uptake, activated Lck and Zap70 colocalize with CD2 in the endosomal fraction on Jurkat T cells that have been activated with anti-CD2 Abs (6). Termination of signaling through internalization of receptor/ligand couples in a large endocytic structure has been described in the interaction between EphB and ephrinB (51,52). Consistent with such resetting of TCR signaling, accumulation of active Zap70 and

phosphotyrosine are transiently suppressed at the center of the interface at 3 min after cell couple formation (53).

Why would T cell signaling benefit from resetting upon cell couple formation? Before encounter of agonist peptide-presenting APCs, low level TCR signaling is critical for T cell homeostasis (54). At the same time, low level TCR signaling has the potential to antagonize stronger, agonistic TCR signals (55). Removal of parts of the TCR signaling machinery through T cell invaginations could remove potentially antagonizing TCR signaling complexes formed in response to prior homeostatic engagement. As not to result in a general attenuation of T cell activation, this resetting should be focused on proximal signaling, as demonstrated in this study. For such a resetting mechanism to function reliably, T cell invaginations have to be sensitive to the affinity of TCR engagement, as also demonstrated in this study. CD2 inclusion would be critical, as even in efficient T cell activation, the number of agonist peptide-MHC complexes on the entire APC surface can be as low as 10 (56). Using the much more prevalent CD2 to CD48 interaction for resetting TCR signaling should make resetting efficient. Physiologically, a significant impact of resetting T cell signaling through T cell invaginations would be limited to situations in which an agonist TCR signal is weak enough to be subject to antagonism in vivo. Although this result is likely rare, it might be important in extending the TCR repertoire to lower affinity TCR MHC-peptide interactions.

Supplementary Material

Refer to Web version on PubMed Central for supplementary material.

Acknowledgments

We thank R. G. W. Anderson and I. Stroynowski (both from the University of Texas Southwestern Medical Center) for helpful discussions; D. J. Fowell (University of Rochester) for T cells from wild-type DO11.10 TCR transgenic mice; R. Y. Tsien (University of California, San Diego) for a plasmid encoding mCherry; A. Sanchez (Stanford University Medical Center) for peptide synthesis; T. Januszewski (University of Texas Southwestern Medical Center) for EM support; K. Luby-Phelps (University of Texas Southwestern Medical Center) for help with deconvolution and spinning disk confocal microscopy; Nicolai S. C. van Oers (University of Texas Southwestern Medical Center) for advice on the biochemistry of T cell signaling; I. Tskvitaria-Fuller for tat-linked dominant-negative Cdc42 and Rac1 proteins; and A. Kulkarni for technical support.

References

1. Davis MM, Boniface JJ, Reich Z, Lyons D, Hampl J, Arden B, Chien Y. Ligand recognition by αβ T cell receptors. Annu. Rev. Immunol 1998;16:523–544. [PubMed: 9597140]
2. Davis SJ, Ikemizu S, Evans EJ, Fugger L, Bakker TR, van der Merwe PA. The nature of molecular recognition by T cells. Nat. Immunol 2003;4:217–224. [PubMed: 12605231]
3. Sprent J. Presidential address to the American Association of Immunologists: stimulating naive T cells. J. Immunol 1999;163:4629–4636. [PubMed: 10528157]
4. Reinherz EL, Chang HC, Clayton LK, Gardner P, Howard FD, Koyasu S, Jin YJ, Moingeon P, Sayre PH. The biology of human CD2. Cold Spring Harb. Symp. Quant. Biol 1989;54(Pt. 2):611–625. [PubMed: 2577023]
5. Meuer SC, Schraven B, Samstag Y. An ‘alternative’ pathway of T cell activation. Int. Arch. Allergy Immunol 1994;104:216–221. [PubMed: 7913355]
6. Marie-Cardine A, Fischer S, Gorvel JP, Maridonneau-Parini I. Recruitment of activated p56^{lck} on endosomes of CD2-triggered T cells, colocalization with ZAP-70. J. Biol. Chem 1996;271:20734–20739. [PubMed: 8702825]
7. Gassmann M, Amrein KE, Flint NA, Schraven B, Burn P. Identification of a signaling complex involving CD2, ζ chain and p59^{fyn} in T lymphocytes. Eur. J. Immunol 1994;24:139–144. [PubMed: 7912674]

8. Breitmeyer JB, Daley JF, Levine HB, Schlossman SF. The T11 (CD2) molecule is functionally linked to the T3/Ti T cell receptor in the majority of T cells. J. Immunol 1987;139:2899–2905. [PubMed: 2444644]
9. Kivens WJ, Hunt SW III, Mobley JL, Zell T, Dell CL, Bierer BE, Shimizu Y. Identification of a proline-rich sequence in the CD2 cytoplasmic domain critical for regulation of integrin-mediated adhesion and activation of phosphoinositide 3-kinase. Mol. Cell Biol 1998;18:5291–5307. [PubMed: 9710614]
10. Nishizawa K, Freund C, Li J, Wagner G, Reinherz EL. Identification of a proline-binding motif regulating CD2-triggered T lymphocyte activation. Proc. Natl. Acad. Sci. USA 1998;95:14897–14902. [PubMed: 9843987]
11. Dustin ML, Olszowy MW, Holdorf AD, Li J, Bromley S, Desai N, Widder P, Rosenberger F, van der Merwe PA, Allen PM, Shaw AS. A novel adaptor protein orchestrates receptor patterning and cytoskeletal polarity in T-cell contacts. Cell 1998;94:667–677. [PubMed: 9741631]
12. Killeen N, Stuart SG, Littman DR. Development and function of T cells in mice with a disrupted CD2 gene. EMBO J 1992;11:4329–4336. [PubMed: 1358605]
13. Purtic B, Pitcher LA, van Oers NS, Wülfing C. T cell receptor (TCR) clustering in the immunological synapse integrates TCR and costimulatory signaling in selected T cells. Proc. Natl. Acad. Sci. USA 2005;102:2904–2909. [PubMed: 15703298]
14. Wülfing C, Sumen C, Sjaastad MD, Wu LC, Dustin ML, Davis MM. Costimulation and endogenous MHC ligands contribute to T cell recognition. Nat. Immunol 2002;3:42–47. [PubMed: 11731799]
15. Wülfing C, Sjaastad MD, Davis MM. Visualizing the dynamics of T cell activation: ICAM-1 migrates rapidly to the T cell:B cell interface and acts to sustain calcium levels. Proc. Natl. Acad. Sci. USA 1998;95:6302–6307. [PubMed: 9600960]
16. Inaba K, Inaba M, Romani N, Aya H, Deguchi M, Ikehara S, Muramatsu S, Steinman RM. Generation of large numbers of dendritic cells from mouse bone marrow cultures supplemented with granulocyte/macrophage colony-stimulating factor. J. Exp. Med 1992;176:1693–1702. [PubMed: 1460426]
17. Tskvitaria-Fuller I, Rozelle AL, Yin HL, Wülfing C. Regulation of sustained actin dynamics by the TCR and costimulation as a mechanism of receptor localization. J. Immunol 2003;171:2287–2295. [PubMed: 12928373]
18. Kolanus W, Nagel W, Schiller B, Zeitlmann L, Godar S, Stockinger H, Seed B. $\alpha_L\beta_2$ integrin/LFA-1 binding to ICAM-1 induced by cytohesin-1, a cytoplasmic regulatory molecule. Cell 1996;86:233–242. [PubMed: 8706128]
19. Yang Z, Vadlamudi RK, Kumar R. Dynein light chain 1 phosphorylation controls macropinocytosis. J. Biol. Chem 2005;280:654–659. [PubMed: 15504720]
20. Monks CR, Freiberg BA, Kupfer H, Sciaky N, Kupfer A. Three-dimensional segregation of supramolecular activation clusters in T cells. Nature 1998;395:82–86. [PubMed: 9738502]
21. Shaner NC, Campbell RE, Steinbach PA, Giepmans BN, Palmer AE, Tsien RY. Improved monomeric red, orange and yellow fluorescent proteins derived from *Discosoma* sp. red fluorescent protein. Nat. Biotechnol 2004;22:1567–1572. [PubMed: 15558047]
22. Randazzo PA, Fales HM. Preparation of myristoylated Arf1 and Arf6 proteins. Methods Mol. Biol 2002;189:169–179. [PubMed: 12094585]
23. Frank S, Upender S, Hansen SH, Casanova JE. ARNO is a guanine nucleotide exchange factor for ADP-ribosylation factor 6. J. Biol. Chem 1998;273:23–27. [PubMed: 9417041]
24. Wild MK, Cambiaggi A, Brown MH, Davies EA, Ohno H, Saito T, van der Merwe PA. Dependence of T cell antigen recognition on the dimensions of an accessory receptor-ligand complex. J. Exp. Med 1999;190:31–41. [PubMed: 10429668]
25. Leupin O, Zaru R, Laroche T, Muller S, Valitutti S. Exclusion of CD45 from the T-cell receptor signaling area in antigen-stimulated T lymphocytes. Curr. Biol 2000;10:277–280. [PubMed: 10712909]
26. Krummel MF, Sjaastad MD, Wülfing C, Davis MM. Differential clustering of CD4 and CD3ζ during T cell recognition. Science 2000;289:1349–1352. [PubMed: 10958781]
27. Conner SD, Schmid SL. Regulated portals of entry into the cell. Nature 2003;422:37–44. [PubMed: 12621426]

28. Amyere M, Mettlen M, Van Der Smissen P, Platek A, Payrastre B, Veithen A, Courtoy PJ. Origin, originality, functions, subversions and molecular signalling of macropinocytosis. Int. J. Med. Microbiol 2002;291:487–494. [PubMed: 11890548]
29. Greenberg S, Grinstein S. Phagocytosis and innate immunity. Curr. Opin. Immunol 2002;14:136–145. [PubMed: 11790544]
30. Donaldson JG. Multiple roles for Arf6: sorting, structuring, and signaling at the plasma membrane. J. Biol. Chem 2003;278:41573–41576. [PubMed: 12912991]
31. Niedergang F, Colucci-Guyon E, Dubois T, Raposo G, Chavrier P. ADP ribosylation factor 6 is activated and controls membrane delivery during phagocytosis in macrophages. J. Cell Biol 2003;161:1143–1150. [PubMed: 12810696]
32. Radhakrishna H, Klausner RD, Donaldson JG. Aluminum fluoride stimulates surface protrusions in cells overexpressing the ARF6 GTPase. J. Cell Biol 1996;134:935–947. [PubMed: 8769418]
33. Langille SE, Patki V, Klarlund JK, Buxton JM, Holik JJ, Chawla A, Corvera S, Czech MP. ADP-ribosylation factor 6 as a target of guanine nucleotide exchange factor GRP1. J. Biol. Chem 1999;274:27099–27104. [PubMed: 10480924]
34. Wadia JS, Dowdy SF. Protein transduction technology. Curr. Opin. Biotechnol 2002;13:52–56. [PubMed: 11849958]
35. Knorr T, Nagel W, Kolanus W. Phosphoinositides determine specificity of the guanine-nucleotide exchange activity of cytohesin-1 for ADP-ribosylation factors derived from a mammalian expression system. Eur. J. Biochem 2000;267:3784–3791. [PubMed: 10848997]
36. Soga N, Namba N, McAllister S, Cornelius L, Teitelbaum SL, Dowdy SF, Kawamura J, Hruska KA. Rho family GTPases regulate VEGF-stimulated endothelial cell motility. Exp. Cell Res 2001;269:73–87. [PubMed: 11525641]
37. Tskvitaria-Fuller I, Seth A, Mistry N, Gu H, Rosen MK, Wülfing C. Specific patterns of Cdc42 activity are related to distinct elements of T cell polarization. J. Immunol 2006;177:1708–1720. [PubMed: 16849480]
38. Leverrier Y, Ridley AJ. Requirement for Rho GTPases and PI3-kinases during apoptotic cell phagocytosis by macrophages. Curr. Biol 2001;11:195–199. [PubMed: 11231156]
39. Marshall JG, Booth JW, Stambolic V, Mak T, Balla T, Schreiber AD, Meyer T, Grinstein S. Restricted accumulation of phosphatidylino-sitol 3-kinase products in a plasmalemmal subdomain during Fcγ receptor-mediated phagocytosis. J. Cell Biol 2001;153:1369–1380. [PubMed: 11425868]
40. Amyere M, Payrastre B, Krause U, Van Der Smissen P, Veithen A, Courtoy PJ. Constitutive macropinocytosis in oncogene-transformed fibroblasts depends on sequential permanent activation of phosphoinositide 3-kinase and phospholipase C. Mol. Biol. Cell 2000;11:3453–3467. [PubMed: 11029048]
41. Navarro-Lérida I, Martinez Moreno M, Roncal F, Gavilanes F, Albar JP, Rodríguez-Crespo I. Proteomic identification of brain proteins that interact with dynein light chain LC8. Proteomics 2004;4:339–346. [PubMed: 14760703]
42. Ghosh-Roy A, Desai BS, Ray K. Dynein light chain 1 regulates dynamin-mediated F-actin assembly during sperm individualization in Drosophila. Mol. Biol. Cell 2005;16:3107–3116. [PubMed: 15829565]
43. Gomez TS, Hamann MJ, McCarney S, Savoy DN, Lubking CM, Heldebrant MP, Labno CM, McKean DJ, McNiven MA, Burkhardt JK, Billadeau DD. Dynamin 2 regulates T cell activation by controlling actin polymerization at the immunological synapse. Nat. Immunol 2005;6:261–270. [PubMed: 15696170]
44. Fiorentini C, Falzano L, Fabbri A, Stringaro A, Logozzi M, Travaglione S, Contamin S, Arancia G, Malorni W, Fais S. Activation of rho GTPases by cytotoxic necrotizing factor 1 induces macropinocytosis and scavenging activity in epithelial cells. Mol. Biol. Cell 2001;12:2061–2073. [PubMed: 11452003]
45. Zhang W, Sloan-Lancaster J, Kitchen J, Trible RP, Samelson LE. LAT: the ZAP-70 tyrosine kinase substrate that links T cell receptor to cellular activation. Cell 1998;92:83–92. [PubMed: 9489702]
46. Lyons DS, Lieberman SA, Hampl J, Boniface JJ, Reay PA, Chien Y, Berg LJ, Davis MM. A TCR binds to antagonist ligands with lower affinities and faster dissociation rates than to agonists. Immunity 1996;5:53–61. [PubMed: 8758894]

47. Hwang I, Huang JF, Kishimoto H, Brunmark A, Peterson PA, Jackson MR, Surh CD, Cai Z, Sprent J. T cells can use either T cell receptor or CD28 receptors to absorb and internalize cell surface molecules derived from antigen-presenting cells. J. Exp. Med 2000;191:1137–1148. [PubMed: 10748232]

48. Patel DM, Arnold PY, White GA, Nardella JP, Mannie MD. Class II MHC/peptide complexes are released from APC and are acquired by T cell responders during specific antigen recognition. J. Immunol 1999;163:5201–5210. [PubMed: 10553040]

49. Borgonovo B, Cocucci E, Racchetti G, Podini P, Bachi A, Meldolesi J. Regulated exocytosis: a novel, widely expressed system. Nat. Cell Biol 2002;4:955–962. [PubMed: 12447386]

50. Tapper H, Furuya W, Grinstein S. Localized exocytosis of primary (lysosomal) granules during phagocytosis: role of Ca^{2+}-dependent tyrosine phosphorylation and microtubules. J. Immunol 2002;168:5287–5296. [PubMed: 11994486]

51. Marston DJ, Dickinson S, Nobes CD. Rac-dependent *trans-en*-docytosis of ephrinBs regulates Eph-ephrin contact repulsion. Nat. Cell Biol 2003;5:879–888. [PubMed: 12973357]

52. Zimmer M, Palmer A, Köhler J, Klein R. EphB-ephrinB bi-directional endocytosis terminates adhesion allowing contact mediated repulsion. Nat. Cell Biol 2003;5:869–878. [PubMed: 12973358]

53. Freiberg BA, Kupfer H, Maslanik W, Delli J, Kappler J, Zaller DM, Kupfer A. Staging and resetting T cell activation in SMACs. Nat. Immunol 2002;3:911–917. [PubMed: 12244310]

54. Stefanova I, Dorfman JR, Tsukamoto M, Germain RN. On the role of self-recognition in T cell responses to foreign antigen. Immunol. Rev 2003;191:97–106. [PubMed: 12614354]

55. Sloan-Lancaster J, Allen PM. Altered peptide ligand induced partial T cell activation: molecular mechanisms and role in T cell biology. Annu. Rev. Immunol 1996;14:1–27. [PubMed: 8717505]

56. Irvine DJ, Purbhoo MA, Krogsgaard M, Davis MM. Direct observation of ligand recognition by T cells. Nature 2002;419:845–849. [PubMed: 12397360]

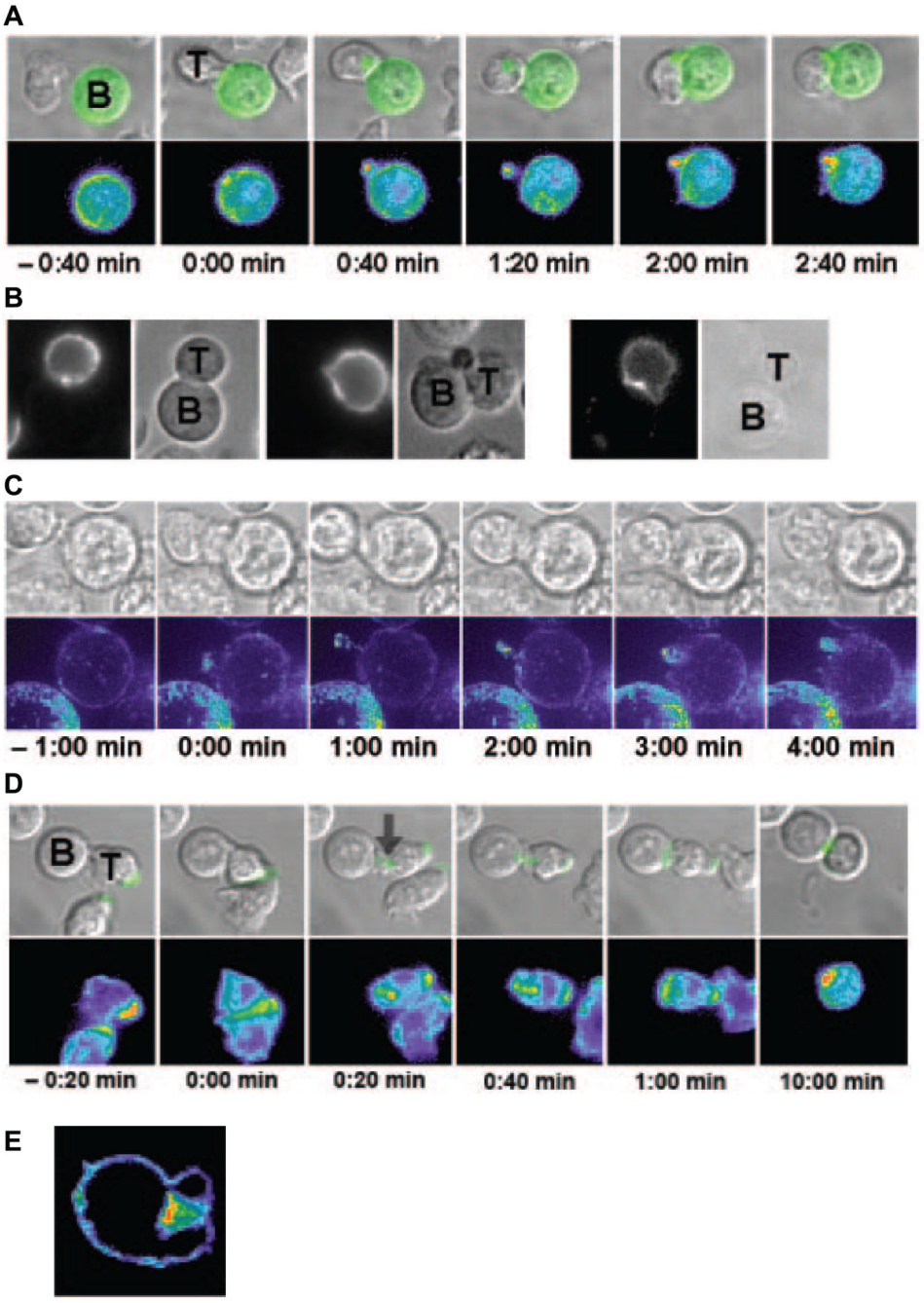

FIGURE 1.

CD48iGFP APC extensions and TCR ζ T cell invaginations. *A*, An interaction of a primary 5C.C7 T cell (T) with a CH27 APC (B) that has been transfected with CD48iGFP in the presence of a full stimulus (10 μM MCC peptide) is shown at the indicated time points relative to tight cell couple formation (*t*= 0:00) in still images. Brightfield images are displayed (*top*) that have been overlaid with the CD48iGFP fluorescence in green. Matching maximum projections (*bottom*) of the three-dimensional CD48iGFP fluorescence intensities in a rainbow false color scale (increasing from purple to red) are shown. Explicit three-dimensional data are shown in Fig. 2. A CD48iGFP extension deep into the T cell can be seen. *B*, Representative anti-CD2 stains of live (*left two*) and fixed (*right*) cell couples between primary 5C.C7 T cells

and CH27 APCs in the presence of a full stimulus are shown. On the *left* of each pair of images, midplane sections of the CD2 fluorescence are given, on the right matching brightfield images. T cells (T) and B cell lymphoma (B) APCs are labeled. Central CD2 accumulation is evident. *C*, Deconvolved fluorescence images of an interaction of a primary 5C.C7 T cell with a CD48iGFP-transfected CH27 cell are shown similar as shown in *A*. *D*, An interaction of a primary DO11.10 T cell (T), transduced with ζ-chain-GFP, with an A20 APC (B) in the presence of a full stimulus (10 μM ova peptide) is shown in still images similar to images shown in *A*. Immediately after cell couple formation (*t*= 0:20 min), central internal ζ-chain-GFP accumulation that is connected to the T cell-APC interface is visible (black arrow). It dissipates subsequently. Stable central TCR accumulation is separate (*t*= 10:00 min). *E*, A single midplane z-section of a ζ-chain-GFP-transduced DO11.10 T cell, activated as in *D*, is shown as acquired on a spinning disk confocal microscope at high magnification. The T cell-APC interface is at the *right* of the cell. A T cell invagination with ζ-chain-GFP accumulation at its base can be seen.

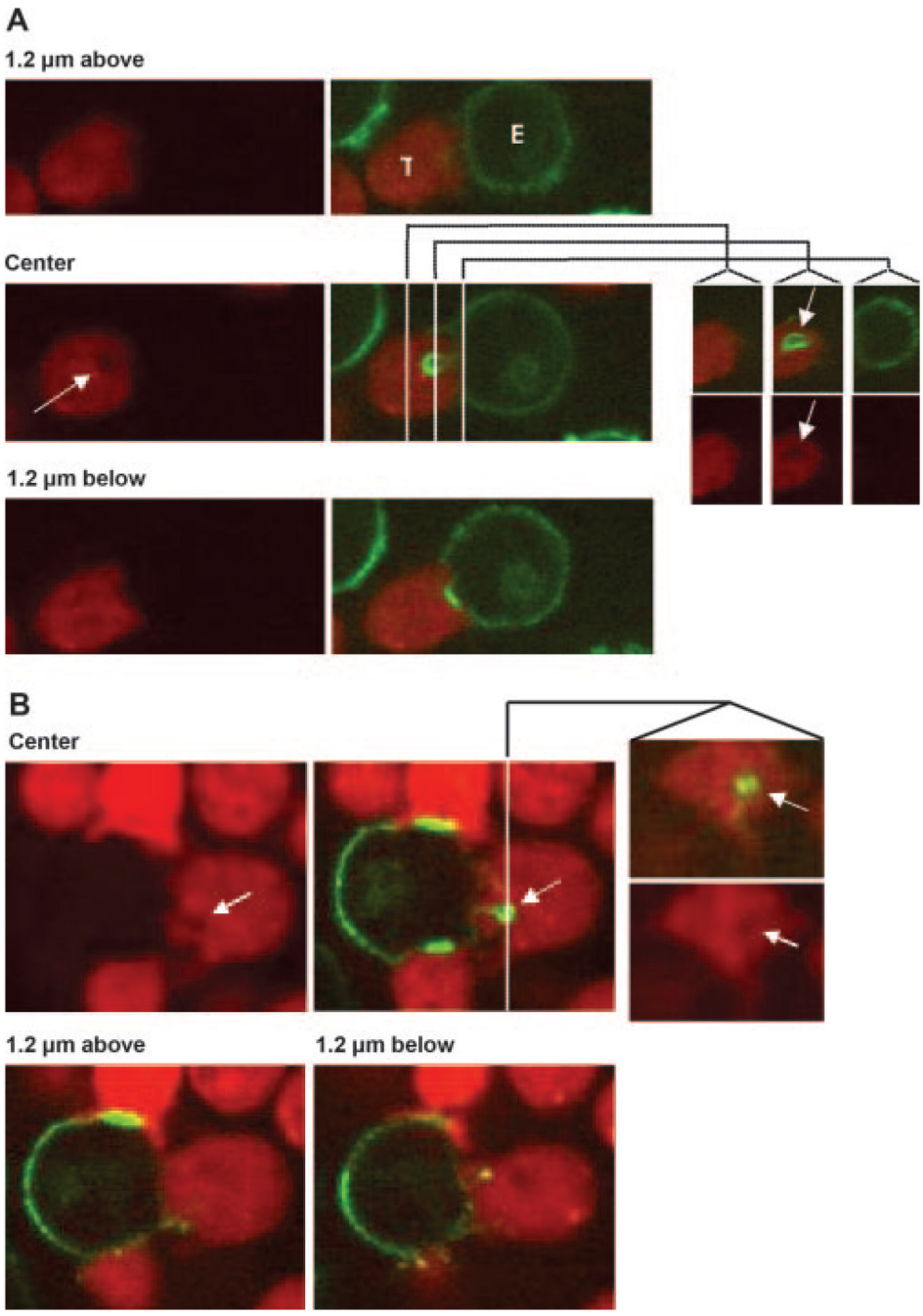

FIGURE 2.

Three-dimensional characterization of T cell invaginations. *A*, A T cell invagination 0.5 min after T cell/APC couple formation using SNARF-labeled primary 5C.C7 T cells (red) and CD48iGFP-transfected CH27 APCs (green) in the presence of a full stimulus (10 µM MCC peptide) is shown. For easier visualization, T cell invaginations were stabilized using 1 µM tat DLC1. Three *xy* cross-sections of the three-dimensional data are shown, 1.2 µm above, at the center of, and 1.2 µm below the invagination, as indicated. SNARF fluorescence only (*left panels*) are presented. A white arrow indicates the position of the CD48iGFP APC extension; a corresponding “hole” in the T cell can be seen. An overlay of the SNARF and GFP fluorescence (*middle panels*) are displayed. Three *yz* cross-sections of the same invagination

event are shown on the *right*. Dotted lines in the central *xy* section indicate the positions of the *yz* sections. *B*, An additional T cell invagination at 0.5 min following T cell/APC couple formation is given similar to *A*.

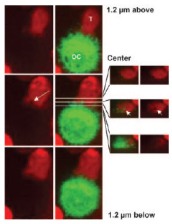

FIGURE 3.

T cell invaginations occur during interactions between T cells and mature DCs. A T cell invagination 0.5 min after T cell/APC couple formation using SNARF-labeled (red) primary 5C.C7 T cells and CFSE-labeled (green) bone marrow-derived mature DCs in the presence of a full stimulus (10 μM MCC peptide) is displayed as in Fig. 2*A*. For easier visualization, T cell invaginations were stabilized using 1 μM tat DLC. In the *xz* sections, as the T cell-APC interface does not lie parallel with the cross-sectional plane, additional APC fluorescence can be seen to the *left* of the invagination event. The invagination event itself, however, is completely surrounded by the T cell and does not protrude out to the side.

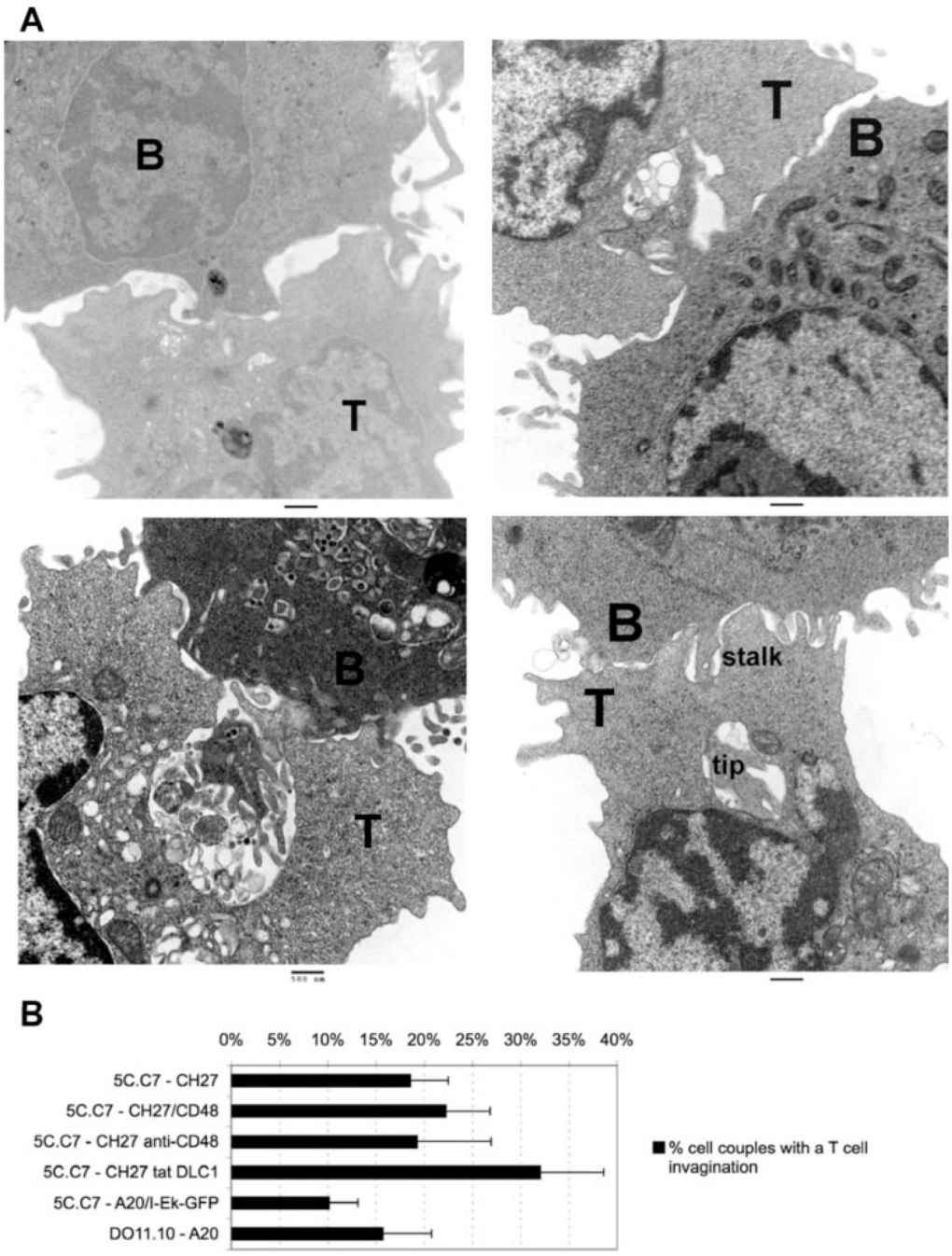

FIGURE 4.

APC extensions and T cell invaginations by EM. *A*, Representative electron micrographs of 5C.C7 T cells that interacted for 2 min with CH27 APCs in the presence of a full stimulus (10 μM MCC peptide) are shown. B cell APCs (B) and T cells (T) are labeled. Scale bar, 0.5 μm. Invaginations range from shallow (*top left*) to intermediate (*top right*) and deep (*bottom right*). The *bottom right* image most likely represents an APC membrane extension with a narrow stalk followed by a wider tip (similar to Fig. 1*C*), as labeled. Part of the stalk is outside the EM section. The *bottom left* image most likely represents a T cell invagination about to close. The image is consistent with beginning degradation of the contents of the invagination. In *B*, The percentage of tight T cell/APC couples with T cell invaginations (as defined in

Materials and Methods) with the SE are given for the indicated T cell and APC combinations. Either 5C.C7 or DO11.10 TCR transgenic T cells were used. APCs had been incubated with 10 μM MCC or OVA peptide, respectively. Anti-CD48 indicates 10 μg/ml anti-CD48 blocking Abs, CD48 indicates transfection with CD48iGFP, and tat DLC1 indicates 1 μM tat DLC1. EM grids were analyzed blind. Twenty-six to 99 (on average 64) cell couples from two or more independent experiments were analyzed per condition.

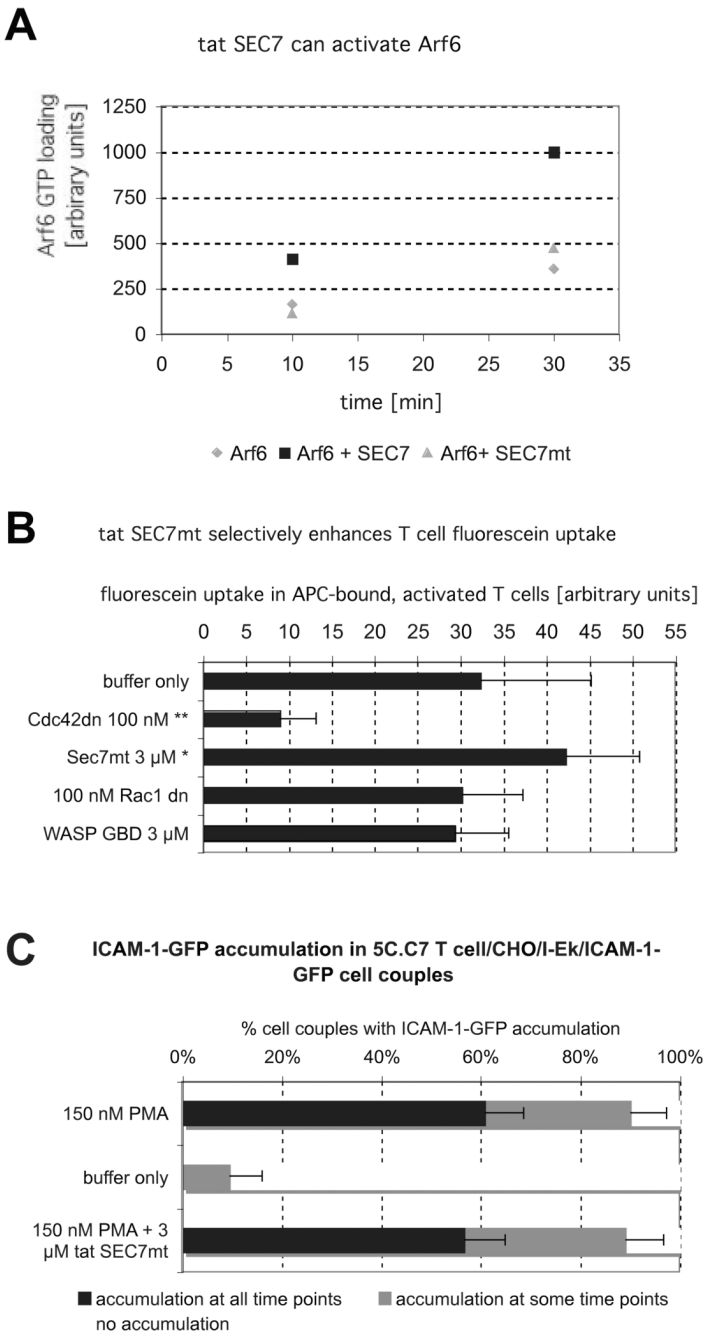

FIGURE 5.

The tat SEC7mt as a reagent to manipulate Arf6 activity. *A*, In vitro GTP loading of purified Arf6 in the presence of 3 µM tat SEC7mt or tat SEC7 is given. One of five representative assays is shown. *B*, Fluid phase uptake of fluorescein into activated APC-bound T cells is given in arbitrary units with SD under the indicated conditions. 5C.C7 T cells were activated with CH27 APC and a full stimulus (10 µM MCC peptide) for 10 min. Statistical significance against buffer only (*, $p < 0.05$ or **, $p < 0.001$) is indicated. Cumulative data of 6–32 experiments per condition with ~20 cells per experiment are shown. Receptor-mediated endocytosis, as measured by transferring uptake, was not substantially affected by 3 µM tat SEC7mt. Uptake enhancement in its presence was 8% (not significant), as opposed to the 31% ($p < 0.05$)

observed for fluid phase uptake. *C*, 5C.C7 T cells were activated by CHO/I-Ek/ICAM-1-GFP APCs in the presence of 10 μM MCC peptide under the indicated conditions. ICAM-1-GFP interface accumulation was analyzed 1, 3, 5, and 7 min after cell couples formation. The percentage of cell couples (with SE) with persistent ICAM-1/LFA-1 accumulation (at all four time points), intermittent accumulation (some (one to three) time points), or no accumulation are given as indicated. Twenty-one to 41 cell couples (33 on average) were analyzed per condition in two or more independent experiments. Statistical significance of differences (using two-sample proportion *z* test) is described in *Results*.

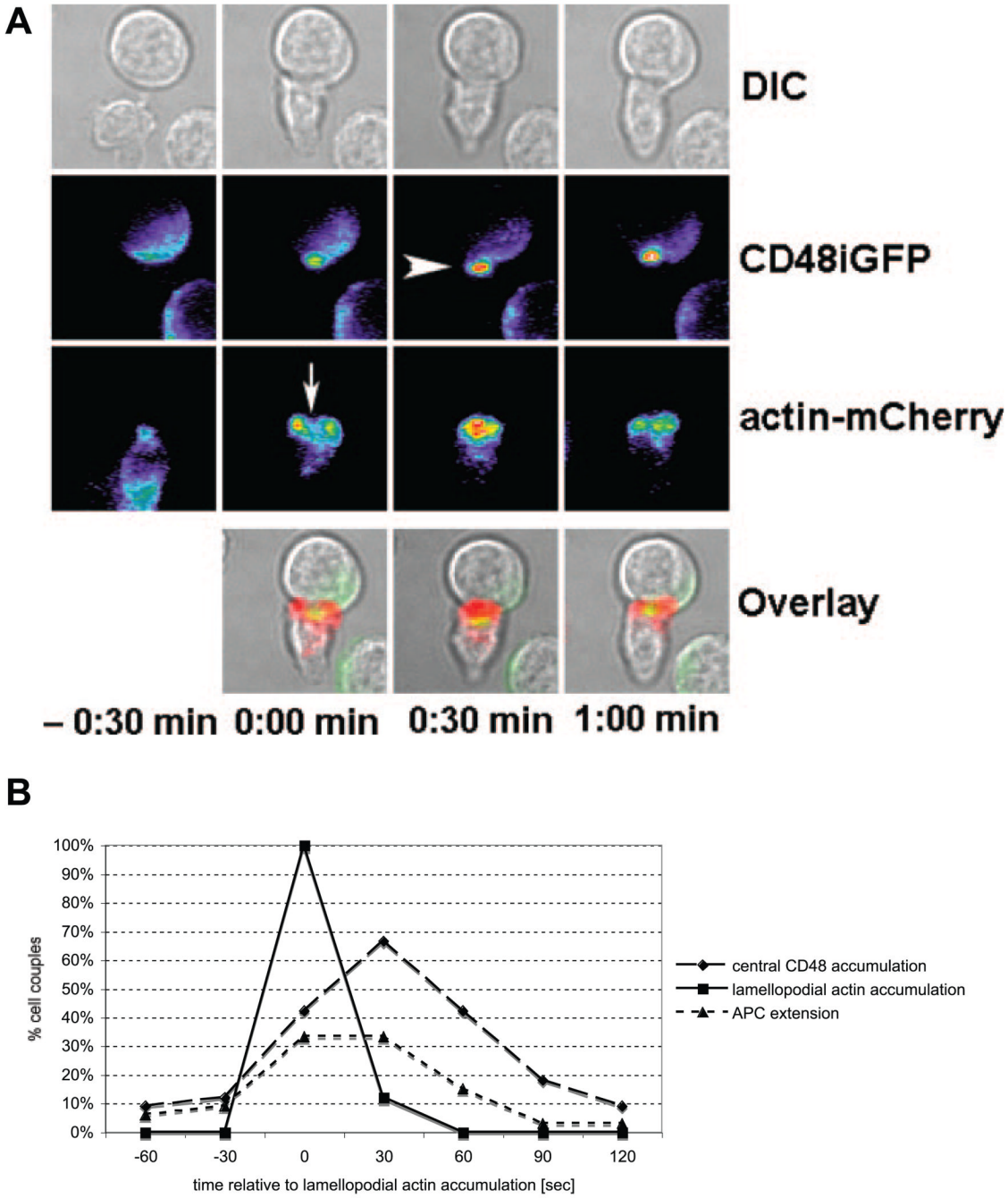

FIGURE 6.

Lamellipodial actin spreading precedes transient central CD48iGFP accumulation and APC extensions. *A*, An interaction of a primary 5C.C7 T cell (T) transduced with actin-mCherry with a CH27 APC (B) that has been transfected with CD48iGFP in the presence of a full stimulus (10 μM MCC peptide) is shown at the indicated time points relative to tight cell couple formation (*t*= 0:00). Differential interference contrast (DIC) brightfield images (*top*) are displayed. Matching maximum projections (*middle*) of the three-dimensional CD48iGFP and actin-mCherry fluorescence intensity are shown in a rainbow false color scale (increasing from purple to red). A white arrow marks the lamellipodial actin spreading, a white arrow head the CD48iGFP APC extension. All data are overlaid (*bottom*) with CD48iGFP fluorescence

(green) and actin-mCherry fluorescence (red). *B*, The dynamics of CD48iGFP central accumulation and APC extensions are shown relative to lamellipodial actin spreading. For each cell couple, the first time point with lamellipodial actin spreading is set to 0. Further lamellipodial actin spreading and CD48iGFP phenotypes are then assessed relative to this time point. The 33 cell couples from two independent groups of experiments are shown.

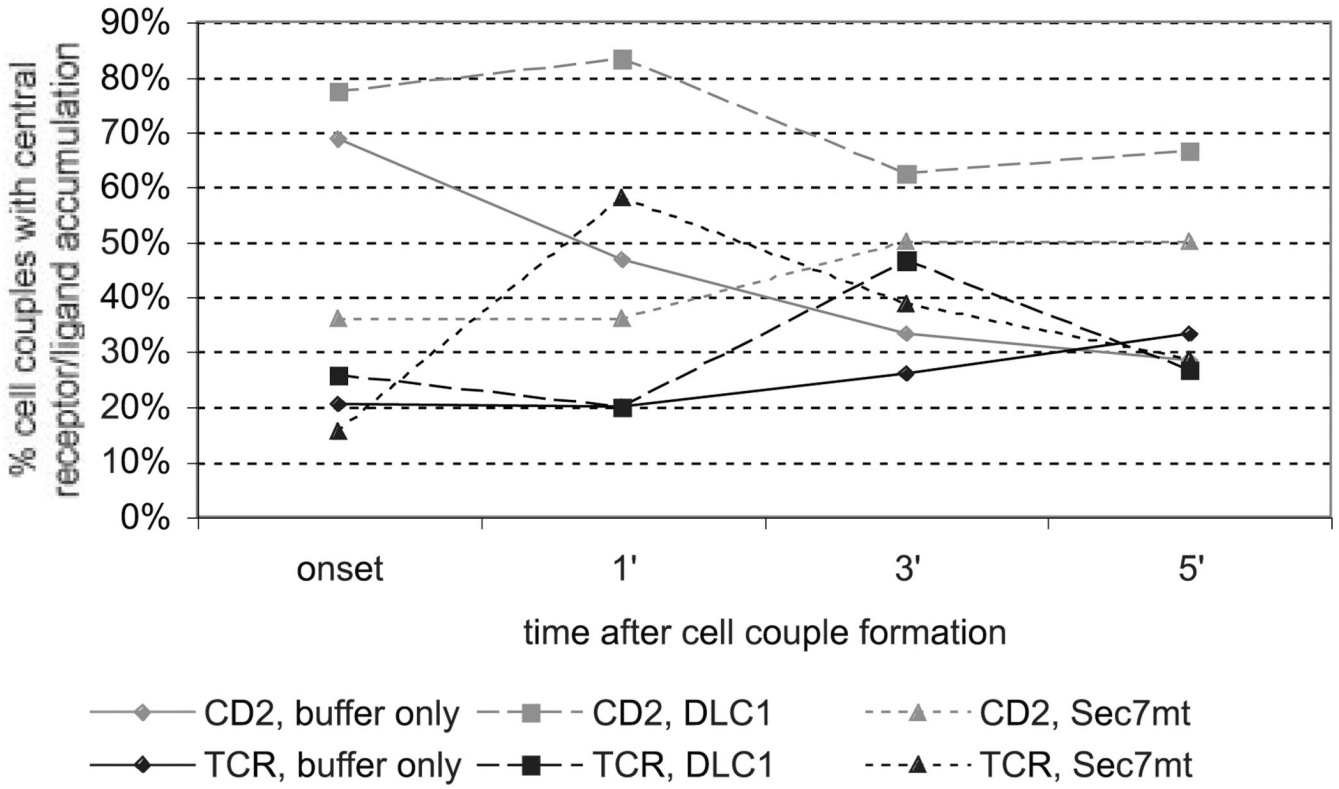

FIGURE 7.

Accumulation of CD2/CD48 at the center of the T cell-APC interface is diminished concomitant with the dissolution of T cell invaginations. The percentage of T cell/APC couples with accumulation of CD2/CD48 or TCR/MHC in a central pattern are given at the indicated time points after cell couple formation in the presence of 1 μM tat DLC1 (DLC1), 3 μM tat SEC7mt (SEC7mt), or buffer only. 5C.C7 T cells and CH27/CD48iGFP (CD2) or A20/I-E^k-GFP (TCR) APCs in the presence of a full stimulus (10 μM MCC peptide) were used. For the time of cell couple formation (onset) the formation of an APC extension is plotted. Twenty-four to 62 (on average 39) cell couples from two or more independent experiments were analyzed. Significance of various data comparisons is given in *Results*.

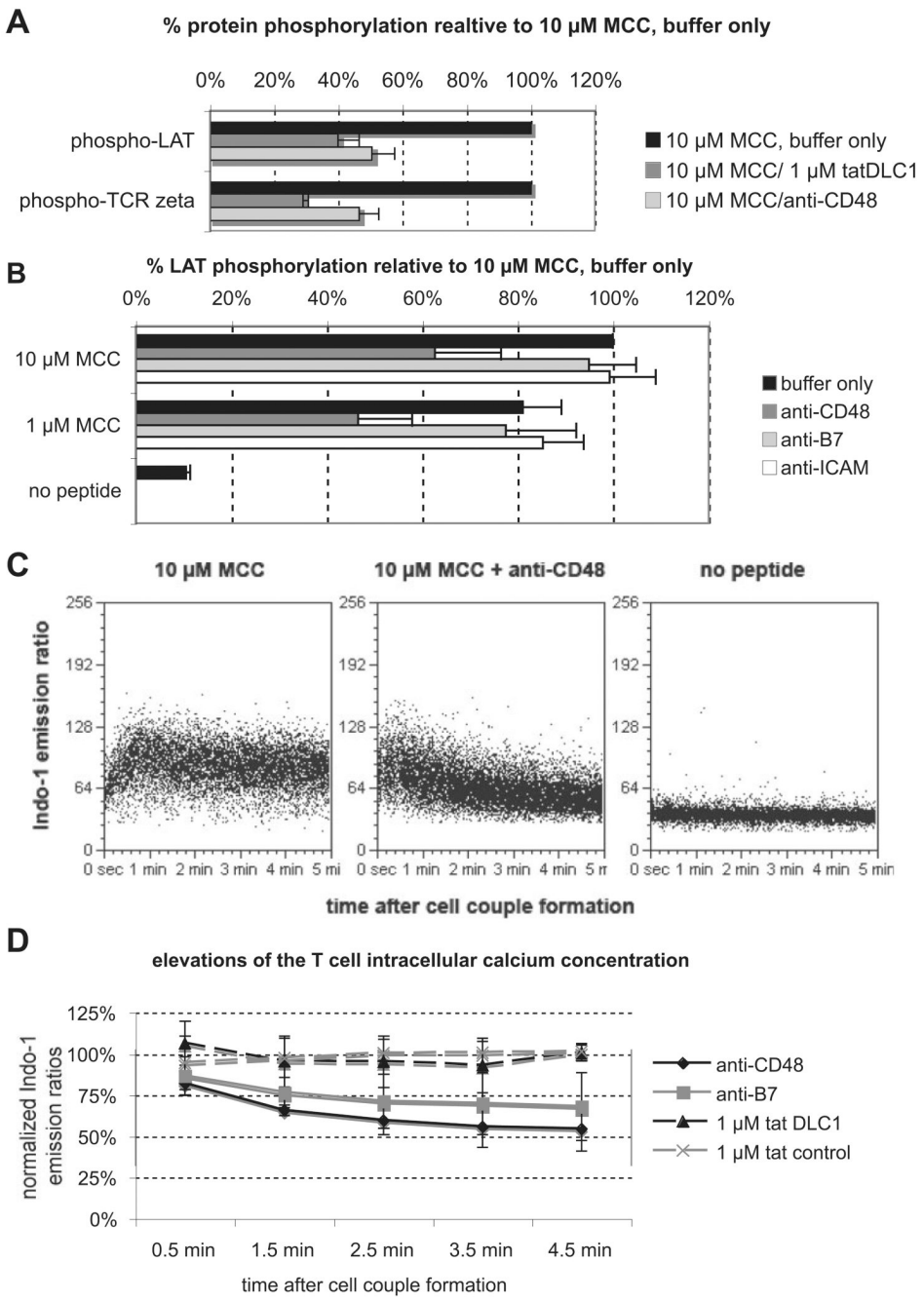

FIGURE 8.

CD2 engagement and dissolution of the T cell invaginations are required for effective proximal TCR signaling. *A*, The amount of phospho-LAT Y191 (as quantified by determination of the band intensity in a Western blot of a whole cell lysate) and that of phospho-TCR-ζ (p21 and p23, as determined by Western blotting of whole cell lysates for phosphotyrosine) is given for 5C.C7 to CH27 interactions after 5 min of cell contact in the presence of 10 μM MCC. The 10 μg/ml anti-CD48 Ab or 1 μM tat DLC1 were present as indicated. Normalized averages (100% is phosphorylation in 5C.C7/CH27 interactions with buffer only) with SD of three independent determinations are shown. *B*, The amount of phospho-LAT Y191 is similarly given for 5C.C7 T cell and A20-I-E^k-GFP APC interactions at the indicated concentration of MCC agonist

peptide. Blocking Abs against CD48, B7-1 plus B7-2, or ICAM-1 were present at 10 μg/ml as designated. Ab treatment did not impair cell couple formation. *C*, Representative flow cytometry plots for the determination of the elevation of the 5C.C7 T cell intracellular calcium concentration are shown. Indo-1-loaded 5C.C7 T cells were gently spun together with CH27 APCs under the indicated conditions and then immediately analyzed by flow cytometry. The emission ratio of Indo-1 is proportional to the T cell intracellular calcium concentration. Plots are gated for 5C.C7 T cells bound to APCs. The percentage of T cells of the total that were bound to APCs in a representative experiment was 19% in the absence of agonist peptide, 39% with a full stimulus (10 μM MCC peptide), 42% with additional anti-B7, 44% with anti-CD48,39% with 1 μM tat peptide, and 41% with 1 μM tat DLC1. Whereas in a single-cell microscopy analysis 40% of T cells contacting an APC bind tightly in the presence of a full stimulus, none do so in the absence of agonist peptide. Likely, not all of the cell couples detected by flow cytometry are thus genuine tight T cell/APC couples. *D*, Normalized data from all experiments are given. The Indo-1 emission ratio for 5C.C7 T cells stimulated with a full stimulus (10 μM MCC peptide) was set to 100%, that for the no peptide condition to 0%. The four experimental conditions shown are a full stimulus with 10 μg/ml anti-CD48, with 10 μg/ml anti-B7-1 and anti-B7-2, with 1 μM tat DLC1, and with 1 μM tat peptide, as indicated. SD is shown. Anti-CD48 data are significantly different from the full stimulus data at all time points with $p \leq 0.05$. Three independent experiments with one to two repetitions of each experimental condition were performed per condition.